Artificial Light at Night of Different Spectral Compositions Differentially Affects Tumor Growth in Mice: Interaction With Melatonin and Epigenetic Pathways

A. E. Zubidat, PhD[1], B. Fares, MSc[2,3], F. Fares, PhD[2,3], and A. Haim, PhD[1]

Abstract

Lighting technology is rapidly advancing toward shorter wavelength illuminations that offer energy-efficient properties. Along with this advantage, the increased use of such illuminations also poses some health challenges, particularly breast cancer progression. Here, we evaluated the effects of artificial light at night (ALAN) of 4 different spectral compositions (500-595 nm) at 350 Lux on melatonin suppression by measuring its urine metabolite 6-sulfatoxymelatonin, global DNA methylation, tumor growth, metastases formation, and urinary corticosterone levels in 4T1 breast cancer cell-inoculated female BALB/c mice. The results revealed an inverse dose-dependent relationship between wavelength and melatonin suppression. Short wavelength increased tumor growth, promoted lung metastases formation, and advanced DNA hypomethylation, while long wavelength lessened these effects. Melatonin treatment counteracted these effects and resulted in reduced cancer burden. The wavelength suppression threshold for melatonin-induced tumor growth was 500 nm. These results suggest that short wavelength increases cancer burden by inducing aberrant DNA methylation mediated by the suppression of melatonin. Additionally, melatonin suppression and global DNA methylation are suggested as promising biomarkers for early diagnosis and therapy of breast cancer. Finally, ALAN may manifest other physiological responses such as stress responses that may challenge the survival fitness of the animal under natural environments.

Introduction

Breast cancer is the most prevailing type of cancer in women and the leading cause of mortality worldwide, except for lung cancer.[1] Breast cancer can result from several causes including genetic and environmental risk factors. Circadian disruption by artificial light at night (ALAN) is relatively a novel risk factor emerging from our modern lifestyle. ALAN is increasingly being related to several diseases and recurrently linked to higher risk of breast cancer among women particularly in urban societies.[2,3] Using geographic information system and questionnaire research, a close and significant association between ALAN and breast cancer was demonstrated in a number of countries including Israel.[4-6]

The association between ALAN and breast cancer also received strong support from experimental studies. In rats, constant ALAN exposure induced the growth of MCF-7 human breast cancer xenografts compared to animals kept under

[1] The Israeli Center for Interdisciplinary Research in Chronobiology, University of Haifa, Haifa, Israel
[2] Department of Human Biology, University of Haifa, Haifa, Israel
[3] Department of Molecular Genetics, Carmel Medical Center, Haifa, Israel

Corresponding Author:
A. E. Zubidat, The Israeli Center for Interdisciplinary Research in Chronobiology, University of Haifa, Haifa, Kiryat Tivon, Israel.
Email: zubidat3@013.net.il

normal light–dark cycle.[7,8] In female BALB/c mice 4T1 mammary carcinoma model, 30 minutes of white fluorescent (450 Lux, 469 nm) or blue light-emitting diode (LED; 350 Lux, 460 nm) ALAN exposures markedly accelerated tumor growth rates compared to ALAN-free controls.[9,10]

The ALAN-induced oncostatic effect is suggested to be manifested by suppressing the typical nocturnal production of the neurohormone melatonin by the pineal gland.[2,11] Melatonin supplement in the drinking water during the night (dark period) significantly blocked the ALAN-accelerated tumor growth in mice.[9,10] Furthermore, breast cancer xenografts treated with nocturnal blood samples collected from premenopausal women exposed to 90 minutes of white fluorescent (2800 Lux) ALAN demonstrated higher tumor proliferative activity than tumors treated with melatonin-rich blood collected during the night period.[12,13] Wavelength induces a dose-dependent suppression of melatonin, with higher frequencies engendering greater suppression compared to lower frequencies.[14] Melatonin is an omnipresent cellular regulator that controls a wide array of cellular processes including gene expression modulation.[15] The exact mechanism of action of melatonin in controlling gene expression is not entirely known, but there is substantial evidence that suggests a link to epigenetic modifications.[16] Certainly, environmental exposures (ie, ALAN) can change gene expression by epigenetic modification that are triggered by hormones (ie, melatonin) and endocrine disruptions.[17]

Epigenetic modifications that modulate gene expression can be manifested by DNA methylation, posttranscriptional regulation of histone proteins, or noncoding RNA silencing.[17,18] DNA methylation is the most common and enduring type of chromatin remodeling that ensue from adding methyl groups at the 5-carbon position of the cytosine base.[19,20] Cancer cells express different types of DNA methylation, including global hypomethylation and promoter hypermethylation of tumor suppressor genes.[21] These aberrant epigenetic modifications induce cancer development probably by stimulating genomic instability, activation of oncogenes, stimulation of metastatic-related genes, silencing tumor suppressor genes, and increasing expression of cell proliferation-related genes.[22] Essentially, the global hypomethylation reported in most cancers is the outcome of decreased methylation in repetitive DNA sequence motifs, which comprise a major proportion of the nuclear DNA.[23,24] Previously methylated genes, particularly oncogenes, can be upregulated in response to demethylation resulting in cellular and genomic instability that may increase carcinogenic potential.[25] Indeed, previous studies have demonstrated that DNA hypomethylation is a major risk factor for activating the expression of pro-metastatic genes.[26-28] In breast cancer, DNA hypomethylation can be detected at early stages of carcinogenesis[29] or can be linked to the tumor differentiation.[30]

The association between ALAN, epigenetics, and cancer development has been previously reviewed.[31] Accordingly, the review suggested that suppression of melatonin levels by ALAN, particularly of short wavelength, might plausibly trigger aberrant DNA methylation, and consequently, carcinogenic

actions are exerted. The association between light pollution and cancer etiology is increasingly being validated by both epidemiological and experimental studies. The problem of light pollution is expected to increase with the extensive increase in LED lighting sources, as higher irradiance and shorter wavelength would be emitted by the new energy-efficient (EE) technology.[32,33] However, little research has been carried out on characterizing the spectral composition and the molecular mechanism of ALAN-induced cancer development. In this study, we exposed 4T1 breast cancer cells-inoculated female BALB/c mice to ALAN emitted from 4 lighting sources with different spectral composition technologies at the same intensity level. Body mass, tumor volume, urinary corticosterone levels, and urinary 6-sulfatoxymelatonin (6-SMT) levels were monitored to characterize the spectral threshold of ALAN on cancer development. Furthermore, global DNA methylation (GDM) levels were also measured in different tissue samples in order to validate a possible mediating molecular connection between ALAN and melatonin suppression with respect to cancer development. We hypothesized that there would be an inverse correlation between ALAN wavelength and tumor growth in which the carcinogenic effect of the suppressed melatonin levels is mediated by decreased GDM levels.

Materials and Methods

Animals

Female BALB/c mice (4-5 weeks, 20 $\pm$ 1 g) were purchased from Harlan Laboratories Ltd (Jerusalem, Israel). The mice were maintained at the Technion Israel Institute of Technology Preclinical Research Authority under specific pathogen-free conditions. All experiments exploiting mice were approved by the Institutional Animal Care and Use Committee of the Technion—Israel institute of Technology, Haifa, Israel (Protocol number: IL-019-01_2011), and all experiment procedures were conducted with approval from the Ethics and Animal Care Committee of the University of Haifa. We made all efforts to minimize the number of animals used and their suffering where no other methods besides using animals were employed. Mice (5/cage) were housed in a climate-controlled room (22°C $\pm$ 1°C, 53% $\pm$ 7% relative humidity) in individually ventilated cages (37 $\times$ 19 $\times$ 13 cm) with 75 changes of air per hour (SmartFlow; Tecniplast, Buguggiate, Italy), given ad libitum access to total pathogen-free food (Altromin 1324, Lage, Germany; 19% crude protein, 4% crude fat, 6% cellulose, 13% moisture, 7.5% ash, and 11.9 MJ/kg metabolizable energy), and sterilized tap water. Prior to tumor cell inoculation, mice were acclimated for 3 weeks to short photoperiod (SD; 8L:16D, light–dark cycle; lights were on between 08:00 and 16:00 hours) emitted from 4 different lightning technologies (carbon [60 W], compact fluorescent lamp [CFL, 12 W], EE-halogen [28 W], and yellow-LED [15 W] at $\lambda_{Dominant}$ = 595 nm, 569 nm, 535 nm, and 500 nm, respectively) at 350 lux. The SD light cycles were interrupted by a 1 $\times$ 30-min/night exposure to ALAN at 00:00 hours using the same light source and spectral

composition as in the light period. Lights were emitted from 2 light fixtures (a single bulb each) that were installed 1 m directly in front of the cages and half a meter apart. For more information, see the study by Zubidat et al.[10] The spectral sensitivity curves of all the lighting technologies tested here are depicted in Supplemental Figure S1.

Cell Culture

4T1 cells originating from transgenic mice were purchased from the American Type Culture Collection (ATCC), a global biosource center, Manassas, Virginia. These are epithelial, p53 wild-type, androgen-dependent, and poorly differentiated cells.[34] The cells were grown in 25- or 75-mL flasks in a humidified incubator at 37°C with 5% CO_2 in Dulbecco modified Eagle medium supplemented with 1.5 mmol/L L-glutamine, 2.2 g/L sodium bicarbonate, 5% fetal bovine serum, and 1% penicillin–streptomycin (all from Biological Industries, Kibbutz Beit Haemek, Israel). For further information, see also the study by Schwimmer et al.[9]

Experiment Protocol

After the acclimation period at a given spectral composition, the mice were inoculated subcutaneously into the hind flank with 1×10^6 (0.2 mL) 4T1 cells and randomly assigned to 2 groups (N = 10 each) in the presence or absence of melatonin (10 mg/L; Sigma, Saint Louis, Missouri) administration in the drinking water (dissolved in 0.01% ethanol). The calculated daily melatonin dose per mouse was 38 μg (1.9 mg/kg/d). Melatonin was given during the dark period (16:00 to 08:00 hours) and substituted by standard sterilized tap water containing bottles during the counterpart light period.

Mice were monitored for body mass and tumor growth twice a week for 1 month and thereafter sampled for urine at 4-hour interval for 28 hours (for determination of 6-SMT and corticosterone levels) and then killed by CO_2 asphyxiation, and tumor, lung, spleen, and liver tissues (for GDM analysis) were immediately removed and stored at –80°C until subsequent analysis. Metastasis nodules in these organs were also inspected visually and recorded. Additionally, spleen mass was recorded immediately after the mice were killed to evaluate correlation with tumor volume (±0.01 g; Ohaus CS200, Parsippany, New Jersey).

Tumor Growth Analysis

Tumor growth was estimated twice a week by measuring the greatest tumor diameters (length and width) using a digital caliber with ±0.01 mm accuracy (Mitutoyo, Kawasaki, Japan). Volume was calculated according to Equation 1.[35]

$$\text{Tumor volume (mm}^3) = \text{Length} \times \text{Width}^2 \times 0.52. \quad (1)$$

Additionally, body mass of the inoculated mice was also recorded throughout the study.

Urine Collection, 6-SMT, and Corticosterone Analysis

Urine. Samples were collected for analyzing both 6-SMT and corticosterone levels. Samples were collected using a noninvasive method for rodents.[36] Mice were housed individually in metabolic cages (Tecniplast, SmartFlow), and urine samples were collected at 4-hour intervals for a period of 28 hours, immediately after the tumor growth measurements. The cage is efficiently designed to collect urine and feces into separate collection tubes. At each collection time, the urine samples were transferred from the collection tubes to 1.5-mL Eppendorf tubes using disposal glass Pasteur pipettes. We calculated urine volume gravimetrically in a tarred 1.5-mL Eppendorf tube by assuming a specific gravity of 1 g/mL.[37] All urine samples were stored at –80°C for further analysis.

6-Sulfatoxymelatonin. Pineal melatonin production levels were determined by measuring urinary 6-SMT concentration, the major metabolite of the hormone.[38,39] The quantitative determination of 6-SMT in urine was completed by a solid-phase enzyme-linked immunosorbent assay (ELISA # RE54031; IBL, Hamburg, Germany) as described previously.[40] Concentrations (ng/mL) of 6-SMT were spectrophotometrically determined by ELISA microplate reader at 450 nm with reference wavelength of 650 nm (PowerWave HT; Biotek, Winooski, Vermont) and analyzed by Gen5 Data Analysis Software (version 2; Biotek).

Corticosterone. Urinary corticosterone concentration was determined using an ELISA kit (ab108821; Abcam, Cambridge, United Kingdom) with 96% recovery for corticosterone, 0.3 ng/mL sensitivity, and 5.0% CV intra-assay variation. Urine samples of 25 μL (diluted 1:20), standards, and reagents were appropriately added to 96-well plates precoated with corticosterone-specific antibody according to the provided instructions. Corticosterone concentrations (ng/mL) were spectrophotometrically determined by ELISA microplate reader at 450 nm, with reference wavelength 570 nm (PowerWave HT; Biotek) and analyzed by Gen5 Data Analysis Software (version 2; Biotek).

Global DNA Methylation Analysis

Genomic DNA was purified from tumor, lung, spleen, and liver cells using High Pure PCR Template Preparation Kit (Roche, Mannheim, Germany). Accordingly, 40 mg tissue samples were lysed at 70°C with proteinase K followed by DNA binding, washing, and eluting according to the instructions of manufacturer. Global DNA methylation was evaluated using the MethylFlash Methylated DNA Quantification Kit (Epigentek, Farmingdale, New York) for analyzing the levels of 5-methylcytosine (5-mC). Purified DNA samples (100 ng) were incubated in 96-well plates coated with 5-mC antibody at 37°C for 90 minutes. After washing, a capture antibody was loaded onto the plates and incubated at room temperature for 30 minutes. Thereafter, the plates were washed and an enhancer solution was added and incubated for 30 minutes at room

temperature. The percentage of methylated DNA was proportional to the optical density at 450 nm. DNA methylation was estimated using positive control (PC; 50% 5 mC) and negative control (NC; 50% unmethylated cytosin) controls according to Equation 2

$$5 - \text{mC} \ (\%) = \frac{(\text{Sample\_OD} - \text{NC\_OD})/\text{S}}{(\text{PC\_OD} - \text{NC\_OD}) \times 2/\text{P}} \times 100, \quad (2)$$

where S is the amount of input DNA (100 ng) and P is the amount of input PC (5 ng). The levels of methylated DNA are calculated as percentage of the total DNA. More information are available in previous studies.[9,10]

Statistical Analysis

All statistical tests were performed using SPSS 13.0 for windows (SPSS Inc, Chicago, Illinois). Three-way mixed repeated-measures analysis of variance (ANOVA; RM3W-ANOVA; 4 spectral compositions × 2 melatonin × 8 time) and 2-way ANOVA (RM2W-ANOVA; 4 spectral compositions × 2 melatonin) with repeated measure were used to evaluate mean value differences in 6-SMT and corticosterone levels between the groups. The effect of the different wavelength treatments on body mass, tumor growth, and GDM levels was analyzed by 2-way ANOVA for mean effects of spectral compositions (4 levels) and melatonin treatment (2 levels). The 2-way and 3-way ANOVAs were followed by 1-way ANOVA if effect of treatment or interactions were statistically significant. The 1-way ANOVA models were followed by Bonferroni and Tukey post hoc pairwise comparisons as appropriate. An independent Student t test was used to determine significant differences between mean levels of experimental variables (eg, tumor growth, body mass, 6-SMT, and GDM) under the different treatments. Relations between 6-SMT, tumor growth, GDM levels, and metastasis formation were assessed by Pearson correlation coefficient (r). Simple linear regression was performed to quantify relationship between wavelength, total 24-hour content of 6-SMT, total 24-hour content of corticosterone, tumor volume, and GDM levels. Linear regression was also used to evaluate the correlation between total 24-hour content of 6-SMT and both tumor volume and GDM levels.

Daily rhythms of urinary 6-SMT concentration levels were also analyzed for rhythmicity using the population cosinor procedure.[41] Accordingly, the data for a given group are modeled by a nonlinear regression to fit the data to the best cosine equation by successive least squares approximation to the complete data over a period of 24 hours using Equation 3:

$$F(t) = \text{Mesor} + \text{Amplitude} \times \cos\left[2\pi \times \frac{(t - \text{Acrophase})}{\text{Period}}\right], \quad (3)$$

where $F(t)$ is 6-SMT concentration at time t, of the best fitted equation described by *Mesor* (rhythm-adjusted mean of the best fitted curve); amplitude, half the difference between maximum and minimum values of the best-fitted curve; acrophase,
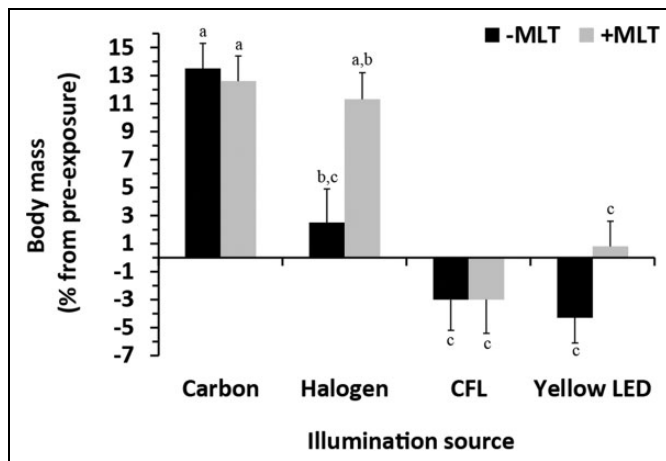

Figure 1. Percentage change in body mass of female BALB/c mice at the end of the study relative to baseline mass prior to tumor cell inoculation (1×10^6 cells). Mice were kept under short photoperiod (8 L:16D, lights were on from 8:00 to 16:00 hours) at 4 different spectral compositions with or without melatonin (MLT) supplement for 28 days. Melatonin was nocturnally administered in the drinking water (10 mg/L). Mice in all spectral groups were exposed to 1×30-minute/night artificial light at night at 00:00 using the same light source and spectral composition as during the day. Results are presented as mean $\pm$ standard error (SE) of n = 6-10. Different letters represent statistically significant difference among groups (Tukey $P = .01$).

the time when the maximum levels occur with reference to 00:00 hours; and period, 24-hour length of a complete cycle. The Jenkins-Watt auto-periodogram analysis was performed to estimate the period of the oscillation.[42] A rhythm is considered significant if the variances of the best-fitted cosine curve and those of the linear model are not equal (F-test statistic at $P < .05$). The population Cosinor analysis was completed by the TSA-Time Series Analysis Serial Cosinor 6.3 software (Expert Soft Technologie, Esvres, France). Data are presented as mean $\pm$ 1 standard error (SE) or 95% confidence interval mean. The statistical error (α) was set at 5% and was corrected for multiple comparisons with a conservative Bonferroni correction. Statistical assumption for linearity and normality was tested by Shapiro-Wilk test, and all assumptions were met for all major analyses. Therefore, no corrections for normality were made.

Results

Body Mass

Artificial light at night of different illumination sources showed a significant effect on the body mass of the 4T1 breast cancer cells-inoculated mice at the end of each experimental trail (1-way ANOVA; $F_{7,61}=15.39$, $P = .0001$). Body mass under both carbon and EE-halogen exposures with or without melatonin supplement showed marked mass gain ($\sim 10\%$) compared to CFL and yellow-LED counterpart exposures where mass loss ($\sim -2\%$) was recorded (Figure 1).

Table 1. Effects of ALAN at 4 Different Spectral Compositions With or Without MLT Supplement on Different Tumor-Related Parameters in 4T1 Breast Cancer Inoculated Female BALB/c Mice.[a]

ALAN Source[b]	MLT	Tumor-Free Interval, days[c]	Tumor Volume, mm^3	Relative Tumor Mass (to Body Mass)	Number of Lung Metastasis[d]	Survival Rate, %
Carbon	−	14	1816 + 284[e]	35 + 4[e,f]	3.3 + 0.6[e]	100
	+		601 + 214[g]	13 + 1[g]	1.2 + 0.5[g]	100
Halogen	−	8	3262 + 163[f]	61 + 6[h]	10 + 0.6[h]	60
	+		1341 + 267[e,g]	24 + 4[e,g]	6 + 0.7[f]	80
CFL	−	7	3391 + 218[c]	51 + 4[c,d]	5.8 + 1.1[e,f]	60
	+		1564 + 248[e,g]	54 + 9[h]	3.7 + 1.2[e]	60
Yellow-LED	−	10	3279 + 211[f]	36 + 3[f]	7.7 + 0.8[f,h]	100
	+		954 + 145[e,g]	18 + 2[g]	3.9 + 1.0[e]	

Abbreviations: ALAN, artificial light at night; CFL, compact fluorescent lamp; LED, light-emitting diode; MLT, melatonin.
[a]Different superscripted letters represent statistically significant difference among groups (Tukey *P* < .05).
[b]Measurements were performed at 4 weeks post tumor cell inoculation.
[c]The duration from 4T1 cells inoculation to the appearance of a measurable tumor.
[d]Visible metastatic nodules on each lung.

Tumor Growth

All of the inoculated mice at the 4 spectral compositions developed visible tumors, but at different days (Table 1). The CFL and EE-halogen exposures were associated with shorter tumor-free intervals (7 and 8 days) compared to yellow-LED and carbon exposures, where the latter exposed-mice showed the longest tumor-free interval (14 days). Carbon and yellow-LED inoculated mice with or without melatonin treatments had a 100% survival rates during 28 days post-inoculation, while the mice exposed to either EE-halogen or CFL ALAN illuminations had worsened survival rates (60%) in both groups with and without melatonin supplement. However, melatonin supplement increased survival rates by 20% only for mice exposed to EE-halogen ALAN (Table 1).

The RM 3-way ANOVA model showed significant time ($F_{7,476} = 225.21$, $P = .0001$), spectral composition ($F_{3,68} = 6.07$, $P = .001$), and melatonin ($F_{1,68} = 52.64$, $P = .0001$) effects on mean tumor growth rates. However, no significant interaction effects were detected between spectral composition and melatonin treatments. All the control groups (without melatonin), except the carbon-inoculated mice, had tumor progression at higher rates than the matched melatonin-treated mice (Figure 2). Mean tumor volume 28 days postinoculation in the carbon control group was about 1.8-fold smaller (1816 + 284 mm^3) than in the other counterpart spectral control groups, which showed no significant differences in mean values. Nocturnal melatonin supplement in the drinking water notably decreased mean tumor volume in all spectral compositions compared to opposite controls. Carbon and yellow-LED-inoculated mice without melatonin showed smaller relative tumor mass to body mass compared to EE-halogen and CFL under the same conditions. Under control conditions, the carbon-exposed mice (3.3 + 0.6 in number) showed the most reduced lung metastases formation, while the most developed formation was detected in the EE-halogen-exposed mice (10 + 0.6 in number). Generally, the melatonin-treated mice in all
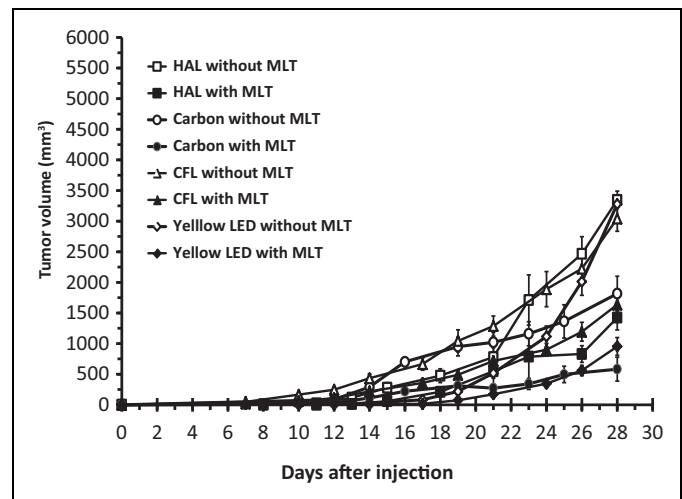

Figure 2. Tumor growth rates of female BALB/c mice during 4 weeks post cancer cell inoculation at 4 different spectral compositions with or without melatonin (MLT) supplement. Tumor volumes were measured by digital caliper semi-weekly. Results are mean ± standard error (SE) of n = 6-10.

spectral groups showed lessened metastases formation compared to controls (Table 1).

Urinary 6-SMT and Corticosterone Levels

Urinary 6-SMT. The 2-way RM-ANOVA detected significant time ($F_{6,174} = 14.42$, $P = .0001$) and spectral composition ($F_{3,29} = 4.64$, $P = .04$) effects on mean urinary 6-SMT concentrations. No interaction effects were detected between time and spectral composition. The time-related effect on 6-SMT was also confirmed by the cosinor analysis. Significant 6-SMT daily rhythms were detected for all examined spectral compositions with 12-hour period under the carbon exposure and 24-hour period the other spectral compositions (Figure 3). The highest mesor was detected under the carbon exposure, whereas the highest amplitude was detected in the
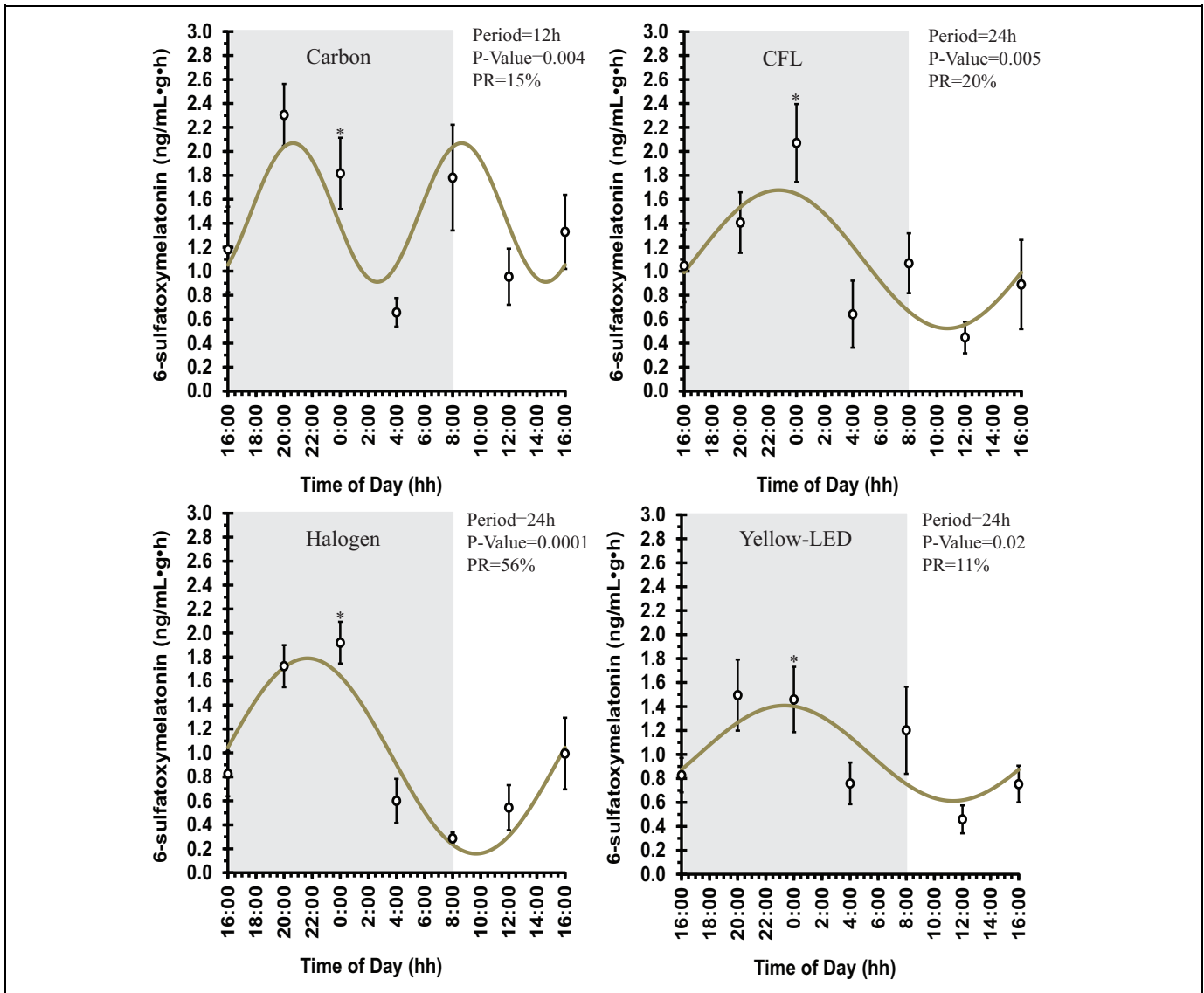
Figure 3. 6-Sulfatoxymelatonin daily rhythms of female BALB/c mice under 4 different spectral compositions (carbon, compact fluorescent lamp [CFL], energy-efficient [EE]-halogen, and Yellow light-emitting diode [LED]) without melatonin treatment 4 weeks postinoculation. Results are mean $\pm$ standard error (SE) of n = 6-10. The best-fitted cosine curve and Cosinor estimates (period, *P* value, and percentage of the rhythm [PR]) are depicted. Gray area in each plot represents the length of the dark period. *P = .03 versus 12:00 hours (*t* test).

EE-halogen-exposed mice. No significant differences were detected between acrophases of all spectral compositions (Supplemental Table S1). Mean daily 6-SMT concentrations of carbon-exposed mice were significantly (Tukey $P < .01$) higher compared to the other spectral compositions. Mean total urinary content of 6-SMT excreted by the carbon-exposed mice over a 28-hour period was significantly different (Tukey $P < .05$) from values detected under all other spectral compositions (302.86 ± 86 ng, 209.12 ± 24.76 nm, 165.66 ± 31.98 ng, and 160.52 ± 29.61 ng for carbon, yellow-LED, EE-halogen, and CFL, respectively).

Urinary corticosterone. Urine concentrations of corticosterone in all spectral groups showed clear daily rhythms over the 28-hour period studied (3WRM-ANOVA; $F_{6,360}=20.18$, $P = .0001$). The ANOVA model also detected spectral composition

($F_{3,60}=84.85$, $P = 0.0001$) and melatonin ($F_{1,60} = 71.18$, $P = .0001$) effects on corticosterone levels, but no interaction effects. Accordingly, clear daily rhythms of urinary corticosterone were also detected by the cosinor analysis at all spectral exposure studied. All rhythms oscillated with a 24-hour period except under the CFL exposure without melatonin where the fitted period was 12 hours (Figure 4). Mesor and amplitude were the lowest in carbon exposure and the highest in yellow-LED exposure, and melatonin supplement significantly decreased mesor levels compared to controls (Supplemental Table S2). Likewise, urinary corticosterone content over a 28-hour period was significantly altered in response to the different spectral exposures (1-way ANOVA, $F_{7,59}=13.81$, $P = 0.0001$). Carbon-exposed mice without melatonin supplement had the lowest 28-hour content (161 ± 22 ng), while the
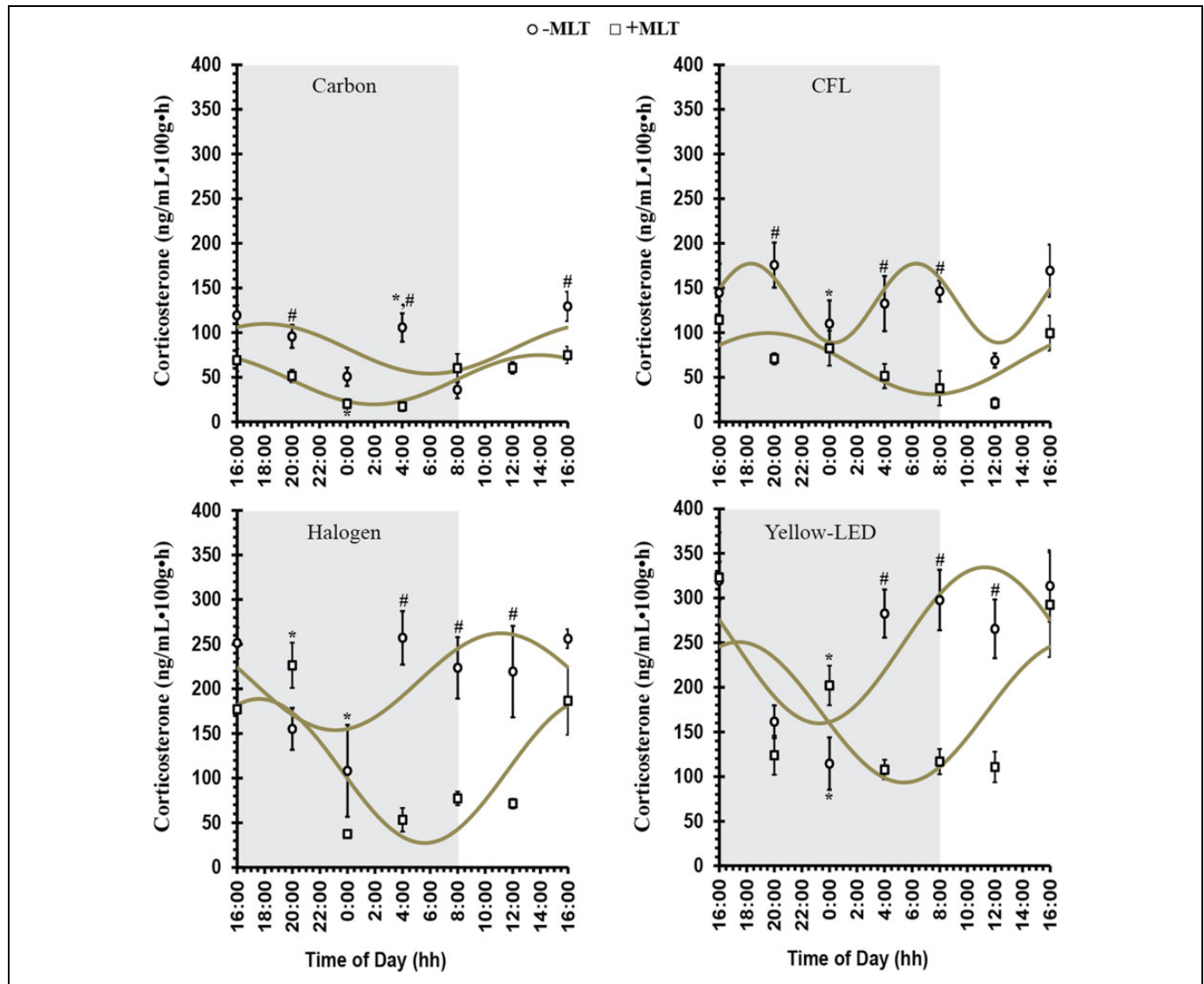
Figure 4. Urinary corticosterone daily rhythms of female BALB/c mice under 4 different spectral compositions with melatonin (+MLT) and without melatonin (−MLT) treatments, 4 weeks post-inoculation. Results are mean ± standard error (SE) of n = 6-10. The best-fitted cosine curve and Cosinor estimates (period, P value, and percentage of the rhythm [PR]) are depicted. Gray area in each plot represents the length of the dark period. *P < .05 versus 12:00 hour and #P < .05 versus +MLT (t test).

highest contents were measured for mice exposed to CFL or yellow-LED (389 ± 24 or 422 ± 58 ng, respectively). The EE-halogen-exposed mice showed intermediate content between these extremes. Melatonin supplement in the drinking water notably decreased the total content of urinary corticosterone in all spectral-exposed mice (Supplemental Figure S2). A simple linear regression analysis revealed a moderate negative correlation between wavelength increment and total content of corticosterone in urine ($r = 0.63$, N = 33, $P = .002$; Supplemental Figure S3).

Levels of GDM

The 3-way RM-ANOVA detected significant tissue ($F_{3,216} = 9.23$, $P = .0001$), spectral composition ($F_{3,72} = 9.23$, $P =$ .0001), and melatonin ($F_{1,72} = 80.68$, $P = 0.0001$) effects on GDM levels, but no interaction effect between melatonin and spectral composition. Generally, all tissues showed marked hypermethylation that was associated with melatonin supplement, while the control groups without melatonin showed hypomethylation (Figure 5). The results revealed tissue-specific response in GDM levels in response to different spectral composition exposures and melatonin treatment. The tumor tissue showed the most prominent changes in GDM levels in response to spectral composition variations and melatonin treatment. The lung GDM levels changed notably in response to spectral composition variations with melatonin supplement, but not without melatonin. In the liver tissue, GDM levels changed only in response to yellow-LED exposure with or without melatonin. In the spleen, no significant differences in
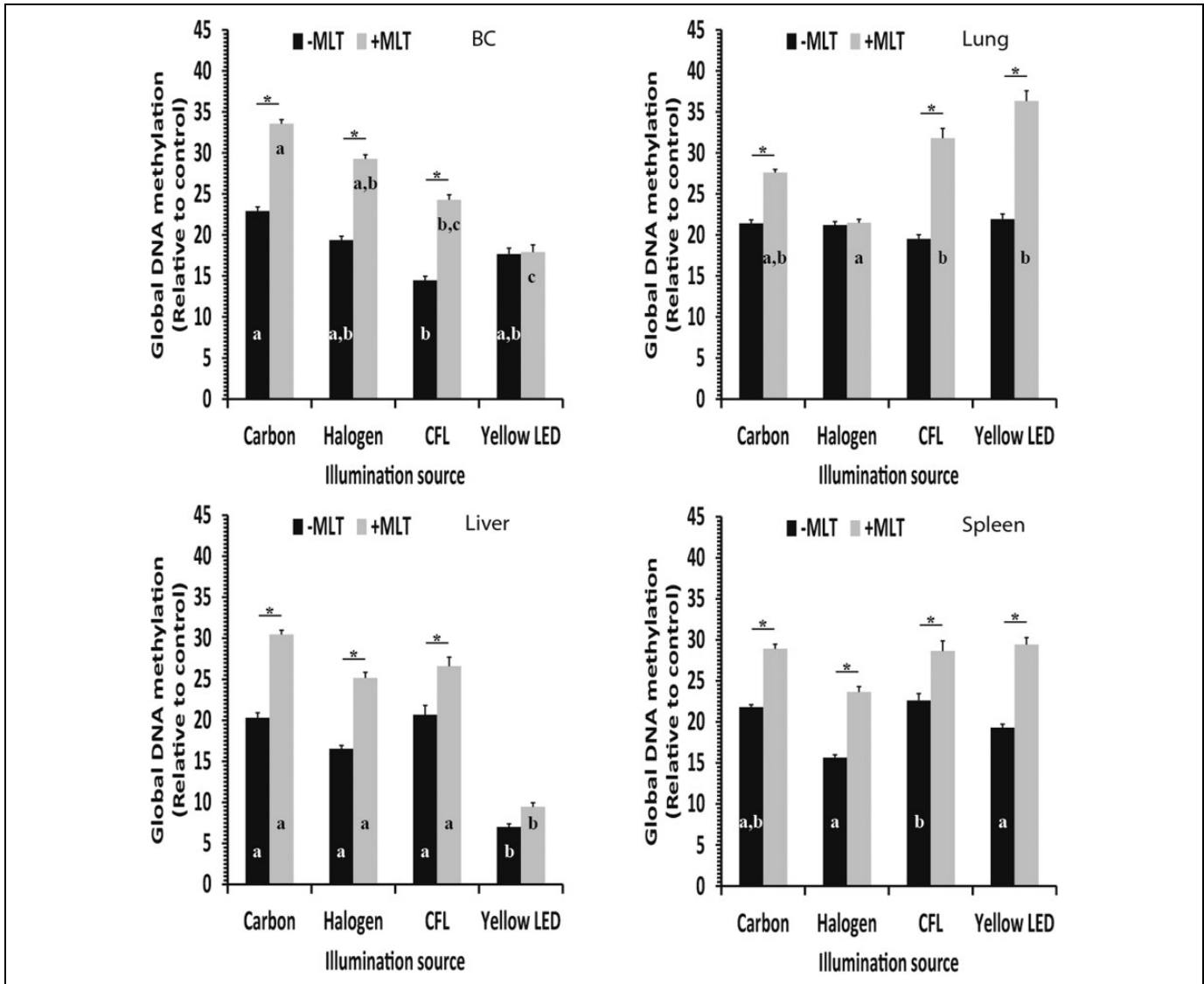
Figure 5. The effects of spectral composition and melatonin (MLT) treatment on global DNA methylation in female BALB/c mice 4 weeks post-inoculation. Results are mean $\pm$ standard error (SE) of n = 10. Different letters represent statistically significant difference among groups within the same tissue and same MLT treatment (Tukey P < .05). * P < .05 (t test).

GDM levels were recorded in response to spectral composition variation with melatonin, but levels changed significantly in the absence of melatonin in the drinking water.

Correlation Analysis

The results showed that total 6-SMT content is closely associated with both tumor volume and GDM levels, but in opposite direction. Tumor volume decreased ($r = -0.8$, N = 33, $P = .0001$), while GDM levels increased ($r = 0.82$, N = 33, $P = .0001$) with increasing 6-SMT content (Figure 6). Additionally, the correlation analysis revealed that tumor volume is positively correlated with relative tumor mass to body mass ($r = 0.62$, N = 67, $P = .0001$), number of lung metastases ($r = 0.63$, N = 67, $P = .0001$), and total urinary corticosterone ($r = .53$, N = 67, $P = .0001$). Finally, wavelength composition

significantly correlated with tumor volume ($r = -0.78$, N = 6, $P = .04$), total content of 6-SMT ($r = 0.75$, N = 6, $P = .04$), and GDM levels ($r = 0.84$, N = 6, $P = .04$; Figure 6).

Discussion

Light pollution is increasingly reported as a potential threat to public health, particularly increased risk of breast and prostate cancers in modern lifestyle.[2] To characterize the spectral threshold of ALAN on breast cancer development, we analyzed the association between increasing spectral composition representing different illumination sources (carbon, EE-halogen, CFL, and yellow-LED) and tumor growth in female BALB/c mice inoculated with 4T1-mice breast cancer cells. Our results discovered a strong inverse correlation between wavelength and both breast cancer burden and metastatic activity. This
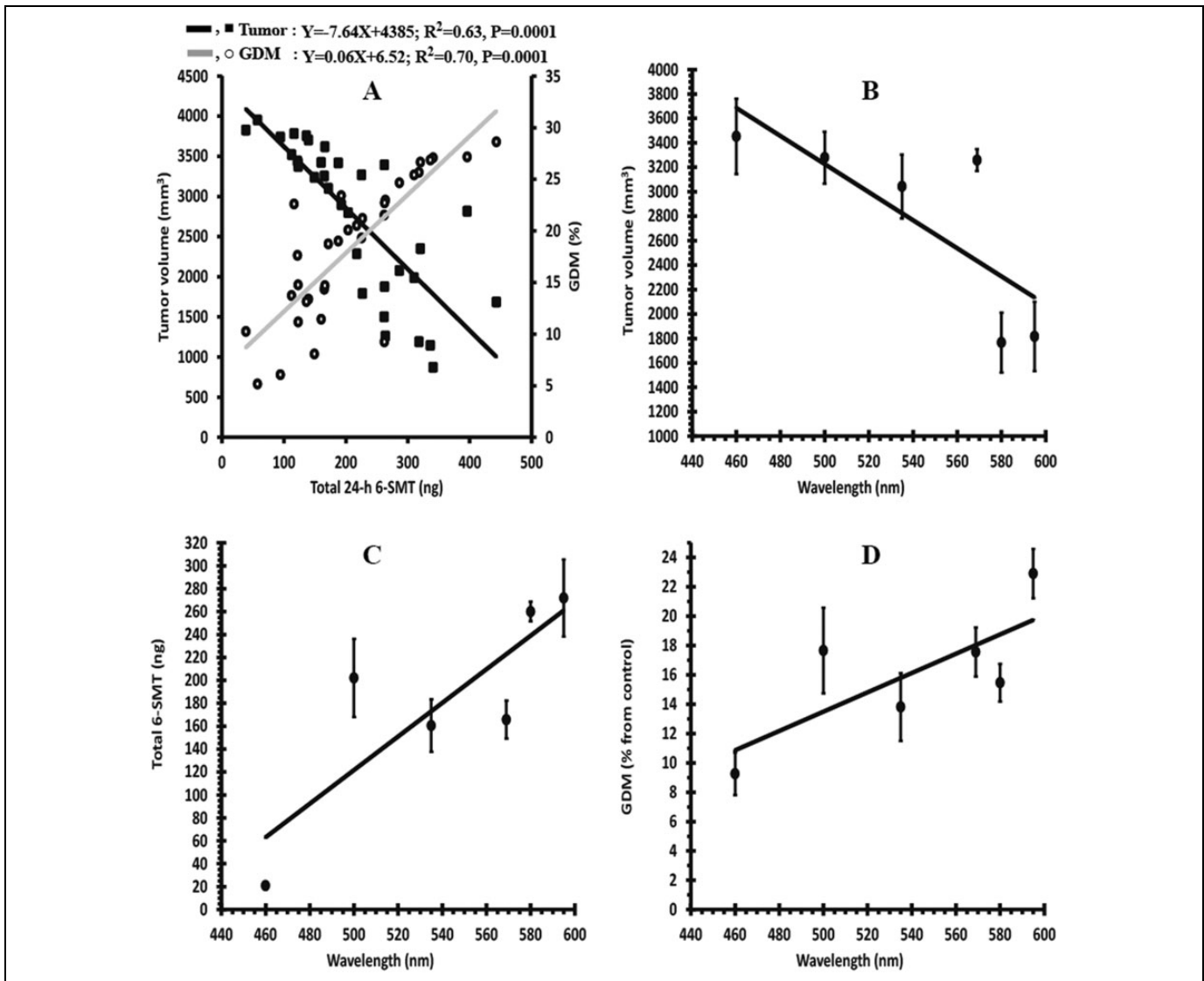
Figure 6. Correlation between various parameters studied in female BALB/c mice 4 weeks post-inoculation with 4T1 breast cancer cells. Regression analysis between total 24-hour content of urinary 6-sulfatoxymelatonin (6-SMT) and both tumor volume and global DNA methylation (GDM). The regression was imposed on the combined data of all spectral groups without melatonin supplement (N = 33). Black and gray solid lines represent the regression lines. The estimated equation, R^2, and P value are also depicted (A). Correlation between wavelength and tumor volume (B), total 6-SMT (C), and GDM (D). Correlations with wavelength were imposed on mean values of control data (without melatonin) at each wavelength. Six wavelengths were used for this analysis: 4 (595, 569, 535, and 500 nm) from the current study and 2 (460 and 580 nm) were adopted from the previous study.[10]

result is consistent with results from our previous work, which revealed a strong association between short wavelength emitted from natural blue LED illumination (460 nm) and tumor growth in a mouse model.[10] In a previous study, tumor growth rates and metastasis formation were most evident under light containing dominant short wavelength compared to long wavelength (580 nm) emitted from incandescent illumination at the same intensity level.

Disruption of circadian rhythms by ALAN might trigger cancer development through suppression of the typical nocturnal rhythm of the pineal hormone melatonin.[3] The oncostatic effects of melatonin are well established. Several studies have

demonstrated that melatonin can prevent the development of breast cancer in animal models.[9,43] Most recently, we have validated in our research center that melatonin supplement in the drinking water of 4T1 tumor-bearing mice suppresses tumor growth and prevents metastases formation in lungs and abdominal organs.[10] In this study, we demonstrated that melatonin can attenuate tumor growth rates and reduce metastases in the lungs of 4T1 tumor-bearing mice at all spectral exposures studied. Further, melatonin can inhibit both tumor growth and metastatic activity in breast cancer cell lines and xenograft.[13,44]

In women with breast cancer, a significant decrease in melatonin levels were noted compared to those of controls.[45-47]

Unequivocally, ALAN exposure particularly of short wavelength suppresses melatonin production and as a possible consequence breast cancer might develop. In this study and previously, we demonstrated a clear dose-dependent suppression of melatonin by wavelength in which short wavelength (eg, blue LED illumination[10]) exposure was the most powerful inhibitor for the pineal hormone. Bright florescent ALAN (580 $\mu W/cm^2$) exposures suppressed melatonin and increased tumor growth in hepatomas and breast cancer xenograft tumor-bearing rats.[12] Furthermore, melatonin-depleted blood collected from women post-ocular ALAN exposure failed to attenuate tumor growth compared to significantly suppressed proliferative activity by melatonin-enriched blood collected during the night.[12] Evidence for a potential association between ALAN exposure and breast cancer risk also comes from epidemiological studies.[48-50]

In a recent Korean study evaluating the spatial effects of ALAN on breast cancer in 25 regions including central, urbanized, and rural areas, a significant correlation was reported between the environmental exposure and increased incidence of breast cancer.[6] The association between ALAN, melatonin suppression, and breast cancer progression appears to be consistent and, even women with blindness or excessive sleepiness (high melatonin levels), presents lower risk compared to normal patients.[51,52]

The oncostatic and antimetastatic properties of melatonin are expected to be mediated by divergent mechanisms including activation of MT1 receptor.[11] In estrogen receptor-related human breast cancer and other mammary malignances, melatonin has been demonstrated to suppress cancer cell proliferation via activation of MT1 receptor.[53-55] Targeting cancer cell metabolism such as blocking linoleic acid uptake and its conversion to 13-hydroxyoctadecadienoic acid via MT1 receptor[56] and other mechanisms, including cell cycle deregulation,[57] blocking Estrogen synthesis,[13] and modulating Rho-associated kinase protein-1-expression,[44] are also suggested to mediate antiproliferative and antimetastatic activities of melatonin.

One of the most promising mechanisms by which melatonin may improve anticancer activities involves epigenetic modifications, particularly DNA hypomethylation.[16] Generally, in breast cancer, decreased DNA methylation can be used as a biomarker for both early detection and staging classification.[28,30] Furthermore, reversal of the aberrant DNA hypomethylation can block breast cancer progression into more aggressive metastatic phenotype.[58] Accordingly, DNA hypomethylation could be used as a novel noninvasive tool for staging and a potential target for therapeutic intervention in breast cancer progression. In this study, we demonstrated a wavelength-dependent decrease in GDM levels and increase in both tumor growth rates and metastases formation in response to 1 × 30-min/night ALAN exposure at midnight. Melatonin supplement in the drinking water was significantly sufficient to increase GDM levels and subsequently lessen the ALAN-induced carcinogenic responses. Melatonin may inhibit tumor development by epigenetic regulation of gene expression. Generally, global hypomethylation and promoter hypermethylation of oncogenes were shown to be involved in regulating carcinogenic activity in breast cancer.[59,60]

Most studies support the idea that these abnormal methylations promote cancer progression by inducing genomic instability, activation of oncogenes (e.g., *breast cancer gene 1; BRCA-1*), silencing tumor suppressor genes, upregulation of metastatic genes, and activation of cell proliferation-related genes.[61] Moreover, in breast cancer, abnormal DNA methylation levels are also suggested to positively correlate with the aggressiveness of metastasis.[62] Melatonin can cause silencing of breast cancer-related oncogenes by changing the methylation pattern of *Aromatase gene* (encoding Estrogen synthetase—a key enzyme for Estrogen biosynthesis) or changing its acetylation pattern.[63] In human breast cancer cell lines, the transcription levels of the oncogenes *EGR3* and *POU4F2/ Brn3b* are lowered by melatonin perfusion, whereas the expression levels of the tumor suppressor gene *GPC3* are elevated by the pineal hormone.[64] Overall, our results suggest that melatonin may induce epigenetic modifications of several cancer-related genes and subsequently regulate silencing or activation of these genes by DNA methylation or other epigenetic pathway. The melatonin-induced hypermethylation in 4T1 tumor-bearing mice suggests a plausible mechanism mediating the association between ALAN wavelength and both tumor growth rates and metastases formation (Figure 7), but the precise molecular processes underlying this correlation remain unexplored and warrant further studies.

The cosinor analysis for 6-SMT revealed significant 24-hour rhythms under all ALAN spectral groups, except under the carbon exposure where a 12-hour ultradian rhythm was detected (Figure 3). We have no clear explanation for 12-hour ultradian rhythm in melatonin secretion detected in the carbon-treated mice. Evidently, carbon illumination has no blue peak at the short wavelength end of the visual spectrum (Supplemental Figure S1), which may account at least partly for the observed ultradian rhythm in our study. Nonetheless, nocturnal ultradian secretory rhythms of melatonin were also reported in both human and rodents.[65,66] In human, the ultradian rhythms in melatonin have been suggested to be associated with rapid eye movement sleep stage, but the significance of these ultradian rhythms in rodent species remains unknown. The detected 12-hour ultradian rhythm in the carbon ALAN-exposed group in this study is characterized by acrophase occurring around the beginning and the end of the dark period. An ultradian rhythm of melatonin secretion with 2 peaks, one in the evening and the other in the morning, has also been reported.[67-69] This bimodal rhythm of melatonin has been suggested to reflect separate regulation of 2 different oscillators. One limitation of this finding in our study is the relatively large sampling time point (4-hour intervals), and thus, higher specimen sampling frequencies are essentially required for more reliable ultradian spectral analysis. The observed dual pattern in melatonin secretion, however, focuses on the complexity of the pineal secretory activity, which most likely is influenced by features of light during the day period.
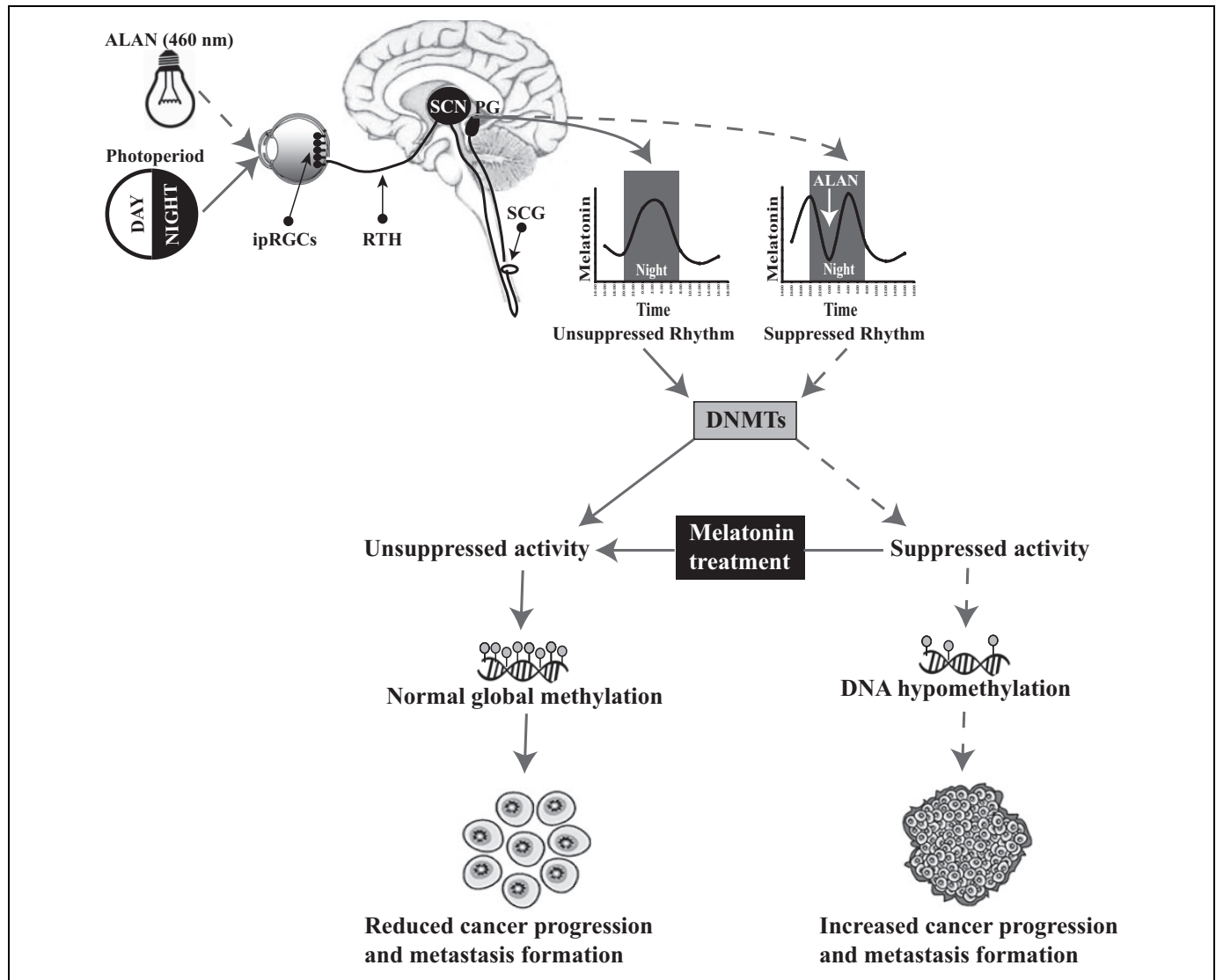
Figure 7. Schematic representation of an epigenetic mechanism of action postulated to mediate cancer progression by artificial light at night (ALAN)-induced melatonin suppression. Photoperiod (day and night cycle) and ALAN signals are detected by intrinsically photosensitive retinal ganglion cells (ipRGCs) and then propagated to circadian clock in the hypothalamic superchiasmatic nucleus (SCN) by the retinohypothalamic tract (RTH). The circadian signals from the SCN are conveyed to the pineal gland (PG) via the superior cervical ganglion (SCG). The SCN-PG pathway regulates normal rhythms of melatonin (solid gray arrows) that are associated with normal activity of DNA methyltransferases (DNMTs), normal global methylation, and finally normal cellular development (cancer free). Conversely, ALAN exposures (solid white arrow and dotted gray arrows) particularly of short wavelengths are associated with converse actions and finally trigger cancer progression and promote metastasis formation. Exogenous melatonin treatment may rectify the ALAN maladaptive responses.

Our results also showed that controlled mice (without melatonin supplement) had increased hypothalamic–pituitary–adrenal axis activity represented by the quantitative increase in urinary corticosterone compared to melatonin-treated mice. Moreover, we discovered an inverse moderate correlation between ALAN wavelength and corticosterone levels, suggesting that ALAN exposure can trigger stress responses in a dose-dependent manner. Previously, we have demonstrated in wild-type rodents a wavelength and irradiance dose-dependent activity of both the sympathetic adrenomedullary system and the hypothalamic–pituitary–adrenal axis.[70] At the cellular level, ALAN exposures have been shown to modulate stress response in the golden spiny mice (*Acomys russatus*), increasing gene expression and protein levels of the heat shock protein 70.[71] Consequently, ALAN exposure (acute not chronic) can trigger physiological processes other than carcinogenic activity that might contribute to fitness and survival under the stressful environmental exposure in wild animals. The wavelength-dependent increase in corticosterone levels is likely to be mediated by the wavelength dose-dependent suppression of melatonin. Generally, melatonin can exert an inhibitory effect on arginine vasopressin rhythms,[72] a major mediator for ACTH release by the pituitary to circulation and subsequently for corticosterone release by the adrenal gland. Our results also

support the suggested inhibitory effect of melatonin on the activity of the hypothalamic–pituitary–adrenal axis as melatonin-treated mice under all spectral compositions showed significant decrease in corticosterone levels compared to control mice (Supplemental Figure S2).

In contrast to the positive effect of acute stress in wild-type animals, chronic stress in humans and animals is also associated with several disorders including breast cancer progression.[73] A systemic review of epidemiological data regarding breast cancer and stress showed a conceivable association between different stressful conditions and breast cancer development.[74] In breast cancer-induced rats that were exposed to social isolation stress, a higher number of tumor and greater volumes were developed compared to group-reared, cancer-induced mice.[75] Furthermore, multiple lines of evidence not only support an association between stressful conditions and cancer development but also with the disease progression and metastasis formation.[76] Our results demonstrated increased tumor development in all spectral groups without melatonin supplement that coincided with higher levels of corticosterone in urine. Conversely, in the melatonin-treated mice, the decreased tumor development corresponded with lower corticosterone levels. These results imply that ALAN exposures could have imposed stressful housing conditions that promoted tumor growth in the melatonin-untreated mice. Although we suggest that increased cancer burden demonstrated here is most likely mediated by melatonin, other mechanisms such as stress responses are plausible.

The Right Lighting Technologies

Here, we attempt to evaluate the spectral composition threshold of ALAN for discrimination between safe and risky lighting technologies, in regard to breast cancer progression. We used different spectral compositions to assess a possible association between ALAN wavelength and melatonin suppression and GDM levels. The 4T1 inoculated-mice were exposed to $1 \times$ 30-min ALAN per night at the same intensity level of each illumination source for 28 nights. Mice were monitored for tumor growth and urinary melatonin to characterize wavelength threshold, the minimal effective wavelength for inducing melatonin suppression, and tumor development. Our results revealed clear negative and positive dose–response relationships between wavelengths, on the one hand, and both tumor growth and urinary 6-SMT levels, on the other, as an indication for pineal melatonin production (Figure 6A and B, respectively). Accordingly, these findings suggest the possibility that tumor growth may be sensitive to wavelength shorter than 500 nm, as ALAN exposures below this threshold correlated with prominent tumor growth, while exposures from this limit and above resulted in markedly reduced tumors. As for melatonin, the most powerful wavelength for suppression of the production levels was 460 nm (natural blue LED), while wavelengths from 580 nm and above exerted very weak melatonin suppression. Wavelengths between 500 and 569 nm showed intermediate suppression effect. The spectral sensitivity curve of all the lighting technologies tested in this study, except for the carbon illumination, demonstrated a peak wavelength at the blue end of the spectrum (Supplemental Figure S2). This peak is responsible for both decreasing the melatonin levels[14] and apparently boosting the tumor progression.

Based on our data, we may conclude that lighting technologies that emit wavelength at 500 nm and longer wavelengths such as carbon illumination and even the traditional incandescent technology could have less health risk than other technologies such as CFL, EE-halogen, and LED lighting, which all present a peak wavelength in the blue region of the spectrum (Supplemental Figure S1). Currently, the LED technology is becoming available at an increasing rate and expected to govern ALAN-lighting in coming years.[33,77] Light-emitting diode lighting exposures are expected to increase the light pollution problem; higher irradiance and shorter wavelength are emitted compared to counterpart traditional options.[32,33] Currently, the LED lighting has almost pervaded every aspect of modern illumination, including outdoor and indoor illuminations, electronic displays, indicator lights, and car lights.[78] With the increased administration of LED lighting for indoor and outdoor illuminations, the need for developing safe and effective illumination sources become more challenging.

Although our results demonstrate clear effect of ALAN of different wavelengths on melatonin suppression, tumor development, and GDM levels, they should be interpreted with some caution. The main caveat arises because the photon flux was not the same for all light sources. However, we are convinced that this limitation had little effect on the overall results, as no substantial differences were detected between photon flux levels estimated at the variant wavelengths that were of relatively narrow range (500-595 nm). Using the irradiance toolbox described previously,[79] we estimated the 30-minute ALAN photon flux at the variant wavelengths measured. The photon flux ranged between 1.06×10^{23} photon/cm^2·second for the shorter wavelength (500 nm) and 1.26×10^{23} photon/cm^2·second for the longest wavelength (595 nm), demonstrating only 16% differences between extremes. Moreover, studies in rodent species demonstrated that the circadian photoreceptive system sensitivity to light exposure decreases with increased time of exposure, as the system integrates the total number of photons over the exposure period.[80] In this study, the mice were exposed to ALAN of only 30 minutes; therefore, no important differences in the effect of the total number of photons detected by the circadian system at the different wavelengths are expected during the brief exposure. Finally, as wavelength increases from 500 to 595 nm, it is expected to emit more infrared photons with less energy (the power of the photon is inversely related to wavelength), which are irrelevant.[81-83] Since all of the light used here are polychromatic with narrow range wavelengths between 500 and 595 nm, the results are more likely to reflect differences in wavelength sensitivity, rather than differences in photon flux. A second limitation in our study design is related to the fact that there is no control group to compare baseline responses in tumor growth,

melatonin suppression, and DNA methylation levels with ALAN-treated groups at the different spectral compositions. Nevertheless, female BALB/c mice as a 4T1 breast tumor model have been used in our research center for over a decade and have become an integral part of our research methodology.[9,10] Baseline responses in the studied variables are well characterized under different spectral compositions, and thus, further mice killing would not add imperative data to our study. Finally, in a more recent study, it has been shown that bright ALAN exposure suppressed melatonin levels, decreased DNA methyltransferase activity, and subsequently reduced GDM compared to controls, and these effects were rectified by melatonin supplement in the drinking water (S. Agbaria, Personal Communication, September 1, 2018).

Conclusions

To the best of our knowledge, our study is the first to demonstrate direct experimental link between spectral composition, melatonin suppression, GDM modification, and mammary tumor growth in a mouse model. We demonstrated a negative correlation between wavelength and melatonin suppression, which is closely associated with increased breast cancer burden. Our data suggest a possible wavelength suppression threshold of 500 nm for melatonin-induced tumor progression. Melatonin suppression and breast cancer burden were most prominent under short-wavelength LED illuminations compared to decreased response under long-wavelength carbon counterpart technology. The results of the current study emphasize the need for developing productive lighting technology that combines the safety of the carbon illumination and the energy efficiency of the LED-matched lighting. This new technology is expected to neutralize or at least lessen the adverse health effects of the chrono disruption of the circadian system, particularly by short-wavelength ALAN. Furthermore, the results of several studies demonstrated that ALAN adverse effects can also be correlated with irradiance levels; therefore, further research is warranted to characterize the irradiance threshold for advancing these adverse effects.

The results also suggest that both melatonin suppression and GDM levels may be utilized as a novel biomarker for cancer progression among key affected populations, particularly night-shift workers. Both markers can be monitored by simple and noninvasive methods and thus may provide significant prevention avenue relying on early detection of risk factor for the malignant illness. Finally, a dose-dependent relationship between wavelength and stress responses revealed here suggests that ALAN may affect other physiological processes that challenge the animal survival fitness such as reproduction and immune responses.

Declaration of Conflicting Interests

The author(s) declared no potential conflicts of interest with respect to the research, authorship, and/or publication of this article.

Supplemental Material

Supplemental material for this article is available online.

References

1. Torre LA, Bray F, Siegel RL, Ferlay J, Lortet-Tieulent J, Jemal A. Global cancer statistics, 2012. *CA Cancer J Clin*. 2015;65(2):87-108.
2. Touitou Y, Reinberg A, Touitou D. Association between light at night, melatonin secretion, sleep deprivation, and the internal clock: health impacts and mechanisms of circadian disruption. *Life Sci*. 2017;173:94-106.
3. Cho Y, Ryu SH, Lee BR, Kim KH, Lee E, Choi J. Effects of artificial light at night on human health: a literature review of observational and experimental studies applied to exposure assessment. *Chronobiol Int*. 2015;32(9):1294-1310.
4. Kloog I, Haim A, Stevens RG, Barchana M, Portnov BA. Light at night co-distributes with incident breast but not lung cancer in the female population of Israel. *Chronobiol Int*. 2008;25(1):65-81.
5. Keshet-Sitton A, Or-Chen K, Yitzhak S, Tzabary I, Haim A. Can avoiding light at night reduce the risk of breast cancer? *Integr Cancer Ther*. 2016;15(2):145-152.
6. Kim YJ, Park MS, Lee E, Choi JW. High incidence of breast cancer in light-polluted areas with spatial effects in Korea. *Asian Pac J Cancer Prev*. 2016;17(1):361-367.
7. Blask DE, Dauchy RT, Sauer LA, Krause JA, Brainard GC. Growth and fatty acid metabolism of human breast cancer (MCF-7) xenografts in nude rats: impact of constant light-induced nocturnal melatonin suppression. *Breast Cancer Res Treat*. 2003;79(3):313-320.
8. Wu J, Dauchy RT, Tirrell PC, et al. Light at night activates IGF-1R/PDK1 signaling and accelerates tumor growth in human breast cancer xenografts. *Cancer Res*. 2011;71(7):2622-2631.
9. Schwimmer H, Metzer A, Pilosof Y, et al. Light at night and melatonin have opposite effects on breast cancer tumors in mice assessed by growth rates and global DNA methylation. *Chronobiol Int*. 2014;31(1):144-150.
10. Zubidat AE, Fares B, Faras F, Haim A. Melatonin functioning through DNA methylation to constrict breast cancer growth accelerated by blue LED light at night in 4T1 tumor bearing mice. *Gratis J Cancer Biol Ther*. 2015;1:57-73.
11. Hill SM, Belancio VP, Dauchy RT, et al. Melatonin: an inhibitor of breast cancer. *Endocr Relat Cancer*. 2015;22(3):R183-R204.
12. Blask DE, Brainard GC, Dauchy RT, et al. Melatonin-depleted blood from premenopausal women exposed to light at night stimulates growth of human breast cancer xenografts in nude rats. *Cancer Res*. 2005;65(23):11174-11184.
13. Blask DE, Hill SM, Dauchy RT, et al. Circadian regulation of molecular, dietary, and metabolic signaling mechanisms of human breast cancer growth by the nocturnal melatonin signal and the consequences of its disruption by light at night. *J Pineal Res*. 2011;51(3):259-269.

14. Falchi F, Cinzano P, Elvidge CD, Keith DM, Haim A. Limiting the impact of light pollution on human health, environment and stellar visibility. *J Environ Manage*. 2011;92(10):2714-2722.

15. Carlberg C. Gene regulation by melatonin. *Ann N Y Acad Sci*. 2000;917:387-396.

16. Hardeland R. Melatonin, noncoding RNAs, messenger RNA stability and epigenetics—evidence, hints, gaps and perspectives. *Int J Mol Sci*. 2014;15(10):18221-18252.

17. Zhang G, Pradhan S. Mammalian epigenetic mechanisms. *IUBMB Life*. 2014;66(4):240-256.

18. Kanherkar RR, Bhatia-Dey N, Csoka AB. Epigenetics across the human lifespan. *Front Cell Dev Biol*. 2014;2:49.

19. Chen T, Li E. Structure and function of eukaryotic DNA methyltransferases. *Curr Top Dev Biol*. 2004;60:55-89.

20. Serman A, Vlahović M, Serman L, Bulić-Jakus F. DNA methylation as a regulatory mechanism for gene expression in mammals. *Coll Antropol*. 2006;30(3):665-671.

21. Dworkin AM, Huang TH, Toland AE. Epigenetic alterations in the breast: implications for breast cancer detection, prognosis and treatment. *Semin Cancer Biol*. 2009;19(3):165-171.

22. Jovanovic J, Rønneberg JA, Tost J, Kristensen V. The epigenetics of breast cancer. *Mol Oncol*. 2010;4(3):242-254.

23. Ehrlich M. DNA hypomethylation in cancer cells. *Epigenomics*. 2009;1(2):239-259.

24. Biscotti MA, Olmo E, Heslop-Harrison JS. Repetitive DNA in eukaryotic genomes. *Chromosome Res*. 2015;23(3):415-420.

25. Wu Y, Sarkissyan M, Vadgama JV. Epigenetics in breast and prostate cancer. *Methods Mol Biol*. 2015;1238:425-466.

26. Pakneshan P, Szyf M, Farias-Eisner R, Rabbani SA. Reversal of the hypomethylation status of urokinase (uPA) promoter blocks breast cancer growth and metastasis. *J Biol Chem*. 2004;279(30):31735-31744.

27. Ogishima T, Shiina H, Breault JE, et al. Increased heparanase expression is caused by promoter hypomethylation and up-regulation of transcriptional factor early growth response-1 in human prostate cancer. *Clin Cancer Res*. 2005;11(3):1028-1036.

28. Loriot A, Van Tongelen A, Blanco J, et al. A novel cancer-germline transcript carrying pro-metastatic miR-105 and TET-targeting miR-767 induced by DNA hypomethylation in tumors. *Epigenetics*. 2014;9(8):1163-1171.

29. Jackson K, Yu MC, Arakawa K, et al. DNA hypomethylation is prevalent even in low-grade breast cancers. *Cancer Biol Ther*. 2004;3(12):1225-1231.

30. Soares J, Pinto AE, Cunha CV, et al. Global DNA hypomethylation in breast carcinoma: correlation with prognostic factors and tumor progression. *Cancer*. 1999;85(1):112-118.

31. Haim A, Zubidat AE. Artificial light at night – melatonin as a mediator between the environment and epigenome. *Philos Trans R Soc Lond B Biol Sci*. 2015;370(1667):20140121.

32. Gaston KJ, Duffy JP, Gaston S, Bennie J, Davies TW. Human alteration of natural light cycles: causes and ecological consequences. *Oecologia*. 2014;176(4):917-931.

33. Kyba CCM, Kuester T, Sanchez de Miguel A, et al. Artificially lit surface of earth at night increasing in radiance and extent. *Sci Adv*. 2017;3(11):e1701528.

34. Foster BA, Gingrich JR, Kwon ED, Madias C, Greenberg NM. Characterization of prostatic epithelial cell lines derived from transgenic adenocarcinoma of the mouse prostate (TRAMP) model. *Cancer Res*. 1997;57(16):3325-3330.

35. Chang L, Huo B, Lv Y, Wang Y, Liu W. Ginsenoside Rg3 enhances the inhibitory effects of chemotherapy on esophageal squamous cell carcinoma in mice. *Mol Clin Oncol*. 2014;2(6):1043-1046.

36. Kurien BT, Everds NE, Scofield RH. Experimental animal urine collection: a review. *Lab Anim*. 2004;38(4):333-361.

37. Schoorlemmer GH, Johnson AK, Thunhorst RL. Circulating angiotensin II mediates sodium appetite in adrenalectomized rats. *Am J Physiol Regul Integr Comp Physiol*. 2001;281(3):R723-R729.

38. de Almeida EA, Di Mascio P, Harumi T, et al. Measurement of melatonin in body fluids: standards, protocols and procedures. *Childs Nerv Syst*. 2011;27(6):879-891.

39. Middleton B. Measurement of melatonin and 6-sulphatoxymelatonin. *Methods Mol Biol*. 2013;1065:171-199.

40. Zubidat AE, Haim A. The effect of alpha- and beta-adrenergic blockade on daily rhythms of body temperature, urine production, and urinary 6-sulfatoxymelatonin of social voles *Microtus socialis*. *Comp Biochem Physiol A Mol Integr Physiol*. 2007;148(2):301-307.

41. Nelson W, Tong Y, Lee J, Halberg F. Methods for cosinor-rhythmometry. *Chronobiologia*. 1979;6(4):305-323.

42. Gouthiere L, Mauvieux B, Davenne D, Waterhouse J. Complementary methodology in the analysis of rhythmic data, using examples from a complex situation, the rhythmicity of temperature in night shift workers. *Biol Rhythm Res*. 2005;36(3):177-193.

43. Melancon K, Cheng Q, Kiefer TL, et al. Regression of NMU-induced mammary tumors with the combination of melatonin and 9-cis-retinoic acid. *Cancer Lett*. 2005;227(1):39-48.

44. Borin TF, Arbab AS, Gelaleti GB, et al. Melatonin decreases breast cancer metastasis by modulating Rho-associated kinase protein-1 expression. *J Pineal Res*. 2016;60(1):3-15.

45. Bartsch C, Bartsch H, Jain AK, Laumas KR, Wetterberg L. Urinary melatonin levels in human breast cancer patients. *J Neural Transm*. 1981;52(4):281-294.

46. Schernhammer ES, Hankinson SE. Urinary melatonin levels and postmenopausal breast cancer risk in the Nurses' Health Study cohort. *Cancer Epidemiol Biomarkers Prev*. 2009;18(1):74-79.

47. Sanchez-Barcelo EJ, Mediavilla MD, Alonso-Gonzalez C, Rueda N. Breast cancer therapy based on melatonin. *Recent Pat Endocr Metab Immune Drug Discov*. 2012;6(2):108-116.

48. Kloog I, Stevens RG, Haim A, Portnov BA. Nighttime light level co-distributes with breast cancer incidence worldwide. *Cancer Causes Control*. 2010;21(12):2059-2068.

49. Bauer SE, Wagner SE, Burch J, Bayakly R, Vena JE. A case-referent study: light at night and breast cancer risk in Georgia. *Int J Health Geogr*. 2013;12:23-33.

50. Rybnikova N, Haim A, Portnov BA. Artificial light at night (ALAN) and breast cancer incidence worldwide: a revisit of earlier findings with analysis of current trends. *Chronobiol Int*. 2015;32(6):757-773.

51. Kliukiene J, Tynes T, Andersen A. Risk of breast cancer among Norwegian women with visual impairment. *Br J Cancer*. 2001; 84(3):397-399.

52. Wu AH, Wang R, Koh WP, Stanczyk FZ, Lee HP, Yu MC. Sleep duration, melatonin and breast cancer among Chinese women in Singapore. *Carcinogenesis*. 2008;29(6):1244-1248.

53. Treeck O, Haldar C, Ortmann O. Antiestrogens modulate MT1 melatonin receptor expression in breast and ovarian cancer cell lines. *Oncol Rep*. 2006;15(1):231-235.

54. Hill SM, Frasch T, Xiang S, Yuan L, Duplessis T, Mao L. Molecular mechanisms of melatonin anticancer effects. *Integr Cancer Ther*. 2009;8(4):337-346.

55. Hill SM, Blask DE, Xiang S, et al. Melatonin and associated signaling pathways that control normal breast epithelium and breast cancer. *J Mammary Gland Biol Neoplasia*. 2011a;16(3): 235-245.

56. Dauchy RT, Blask DE, Dauchy EM, et al. Antineoplastic effects of melatonin on a rare malignancy of mesenchymal origin: melatonin receptor-mediated inhibition of signal transduction, linoleic acid metabolism and growth in tissue-isolated human leiomyosarcoma xenografts. *J Pineal Res*. 2009;47(1):32-42.

57. Cos S, Blask DE, Lemus-Wilson A, Hill AB. Effects of melatonin on the cell cycle kinetics and "estrogen-rescue" of MCF-7 human breast cancer cells in culture. *J Pineal Res*. 1991;10(1):36-42.

58. Szyf M. DNA methylation signatures for breast cancer classification and prognosis. *Genome Med*. 2012;4(3):26-38.

59. Hill VK, Ricketts C, Bieche I, et al. Genome-wide DNA methylation profiling of CpG islands in breast cancer identifies novel genes associated with tumorigenicity. *Cancer Res*. 2011b;71(8): 2988-2999.

60. Saelee P, Chaiwerawattana A, Ogawa K, Cho YM, Tiwawech D, Suktangman V. Clinicopathological significance of BRCA1 promoter hypermethylation in thai breast cancer patients. *Asian Pac J Cancer Prev*. 2014;15(24):10585-10589.

61. Xiang TX, Yuan Y, Li LL, et al. Aberrant promoter CpG methylation and its translational applications in breast cancer. *Chin J Cancer*. 2013;32(1):12-20.

62. Byler S, Goldgar S, Heerboth S, et al. Genetic and epigenetic aspects of breast cancer progression and therapy. *Anticancer Res*. 2014;34(3):1071-1077.

63. Korkmaz A, Sanchez-Barcelo EJ, Tan DX, Reiter RJ. Role of melatonin in the epigenetic regulation of breast cancer. *Breast Cancer Res Treat*. 2009;115(1):13-27.

64. Lee SE, Kim SJ, Yoon HJ, et al. Genome-wide profiling in melatonin-exposed human breast cancer cell lines identifies differentially methylated genes involved in the anticancer effect of melatonin. *J Pineal Res*. 2013;54(1):80-88.

65. Chan YS, Cheung YM, Pang SF. Rhythmic release pattern of pineal melatonin in rodents. *Neuroendocrinology*. 1991;53(suppl 1):60-67.

66. Geoffriau M, Claustrat B, Veldhuis J. Estimation of frequently sampled nocturnal melatonin production in humans by deconvolution analysis: evidence for episodic or ultradian secretion. *J Pineal Res*. 1999;27(3):139-144.

67. Wehr TA, Schwartz PJ, Turner EH, Feldman-Naim S, Drake CL, Rosenthal NE. Bimodal patterns of human melatonin secretion consistent with a two-oscillator model of regulation. *Neurosci Lett*. 1995;194(1-2):105-108.

68. Nakahara D, Nakamura M, Iigo M, Okamura H. Bimodal circadian secretion of melatonin from the pineal gland in a living CBA mouse. *Proc Natl Acad Sci USA*. 2003;100(16):9584-9589.

69. Zubidat AE, Nelson RJ, Haim A. Photosensitivity to different light intensities in blind and sighted rodents. *J Exp Biol*. 2009; 212(Pt 23):3857-3864.

70. Zubidat AE, Nelson RJ, Haim A. Spectral and duration sensitivity to light-at-night in 'blind' and sighted rodent species. *J Exp Biol*. 2011;214(Pt 19):3206-3217.

71. Ashkenazi L, Haim A. Light interference as a possible stressor altering HSP70 and its gene expression levels in brain and hepatic tissues of golden spiny mice. *J Exp Biol*. 2012;215(Pt 22): 4034-4040.

72. Juszczak M, Bojanowska E, Dabrowski R. Melatonin and the synthesis of vasopressin in pinealectomized male rats. *Proc Soc Exp Biol Med*. 2000;225(3):207-210.

73. Antonova L, Aronson K, Mueller CR. Stress and breast cancer: from epidemiology to molecular biology. *Breast Cancer Res*. 2011;13(2):208-223.

74. Chiriac VF, Baban A, Dumitrascu DL. Psychological stress and breast cancer incidence: a systematic review. *Clujul Med*. 2018; 91(1):18-26.

75. De la Roca-Chiapas JM, Barbosa-Sabanero G, Martínez-García JA, et al. Impact of stress and levels of corticosterone on the development of breast cancer in rats. *Psychol Res Behav Manag*. 2016;9:1-6.

76. Moreno-Smith M, Lutgendorf SK, Sood AK. Impact of stress on cancer metastasis. *Future Oncol*. 2010;6(12):1863-1881.

77. Schubert EF, Kim JK. Solid-state light sources getting smart. *Science*. 2005;308(5726):1274-1278.

78. Tosini G, Ferguson I, Tsubota K. Effects of blue light on the circadian system and eye physiology. *Mol Vis*. 2016;22:61-72.

79. Lucas RJ, Peirson SN, Berson DM, et al. Measuring and using light in the melanopsin age. *Trends Neurosci*. 2014;37(1):1-9.

80. Comas M, Beersma DG, Spoelstra K, Daan S. Circadian response reduction in light and response restoration in darkness: a "skeleton" light pulse PRC study in mice (Mus musculus). *J Biol Rhythms*. 2007;22(5):432-444.

81. Figueiro MG, Rea MS. The effects of red and blue lights on circadian variations in cortisol, alpha amylase, and melatonin. *Int J Endocrinol*. 2010;2010:829351. doi:10.1155/2010/829351.

82. Chellappa SL, Steiner R, Blattner P, Oelhafen P, Götz T, Cajochen C. Non-visual effects of light on melatonin, alertness and cognitive performance: can blue-enriched light keep us alert? *PLoS One*. 2011;6(1):e16429. doi:10.1371/journal.pone.0016429.

83. Fonken LK, Nelson RJ. The effects of light at night on circadian clocks and metabolism. *Endocr Rev*. 2014;35(4):648-670.